frontiers | Frontiers in Materials

TYPE Original Research
PUBLISHED 08 November 2023
DOI 10.3389/fmats.2023.1224883

OPEN ACCESS

EDITED BY
Zhi Li,
Central South University, China

REVIEWED BY
Sathish Kumar Palaniappan,
King Mongkut's University of Technology North Bangkok, Thailand
Khubab Shaker,
National Textile University, Pakistan

*CORRESPONDENCE
Jie Li,
101014@hrbcu.edu.cn

RECEIVED 18 May 2023
ACCEPTED 22 September 2023
PUBLISHED 08 November 2023

CITATION
Liu Y, Wang D and Li J (2023), Polyimide aerogel/aramid fiber composite with high mechanical strength and thermal insulation for thermal protective clothing. *Front. Mater.* 10:1224883.
doi: 10.3389/fmats.2023.1224883

Polyimide aerogel/aramid fiber composite with high mechanical strength and thermal insulation for thermal protective clothing

Yuhang Liu[1], Donglin Wang[2] and Jie Li[3]*

[1]Management School, Harbin University of Commerce, Harbin, Heilongjiang, China, [2]College of Engineering, China Agricultural University, Beijing, China, [3]School of Energy and Construction Engineering, Harbin University of Commerce, Harbin, Heilongjiang, China

Polyimide (PI) aerogel, as a new organic aerogel material, has the excellent thermal properties of polyimide and the characteristic of high thermal insulation of aerogels, and has gained increasing attention. In this work, using PI aerogel as the matrix material and aramid fiber as the reinforcement material, controllable flexible PI aerogel/aramid fiber composite insulation materials were successfully prepared by freeze-drying and soft treatment. This study sought to determine how the mass percentage of PI aerogel affected the microstructure, mechanical characteristics, thermal insulation capabilities, and thermal comfort of clothes in PI aerogel/aramid fiber composites. To achieve this, the preparation process of PI aerogel was optimized, and the effects of different mass fractions of PI aerogel on the properties of the composite material were evaluated. The results demonstrated that increasing the mass fraction of PI aerogel led to improvements in the mechanical properties, flexibility, and heat insulation properties of the composite material. Furthermore, the PI aerogel/aramid fiber composite offered enhanced thermal comfort to the wearer in hot and humid environments, indicating that the composite material is particularly suited for thermal insulation applications.

KEYWORDS

polyimide aerogel, aramid fiber, thermal insulation, thermal protective clothing, thermal comfort

1 Introduction

Aerogel is a kind of three-dimensional nano-porous material with ultra-high porosity (Ze et al., 2018a). A large number of nano-sized pores in aerogel gives it the characteristics of low density, low refractive index, small aperture, high specific surface area, and high porosity, which makes aerogel have good light transmission, environmental protection, sound insulation, and other properties (Lee et al., 2011; Ivanov and Ivanov, 2014; Du and Kim, 2022; Stan et al., 2022). Due to the porosity of up to 90%, the aerogel material mainly conducts heat in the gaseous phase, which possesses high thermal insulation and high surface area. The impressive thermal insulation property of aerogels lends itself to diversified applications where heat insulation is crucial, such as in aerospace, building retrofitting, industry for cryogenic applications, cold weather outdoor gear (Laskowski et al., 2015; Adhikary et al., 2021; Cao and Yuan, 2021; Lee et al., 2018; Lei et al., 2018; Zhang et al., 2020). The aerogel material has excellent thermal insulation performance, which makes it a research hotspot in the field of thermal clothing (Liu et al., 2022). However, the extensive application

of traditional inorganic silicon aerogel is restricted by its fragility. Therefore, finding ways to improve the flexibility and structural stability of aerogel materials is a hot topic at present. Du and Kim (2019) added SiO_2 aerogel powder into the flexible polyimide foam material so that the aerogel material was evenly distributed on the wall of the bubble hole, increasing its flexibility and avoiding serious problems such as powder loss (Dai et al., 2021). At the same time, the thermal conductivity of the aerogel insulation layer prepared can be as low as 0.026 W/(m·k), which can meet the needs of heat preservation and insulation (Lei et al., 2006; Ageev and Ponomarev, 2018).

To overcome the problem associated with aerogel brittleness, polyimide (PI) aerogel, as a new organic aerogel material, is gradually gaining attention. Polyimide refers to a class of macromolecular chemicals with imide rings on their molecular chains (Zhang et al., 2018). Due to the stability of their molecular structure, polyimide materials have excellent mechanical properties and thermal stability (Fan et al., 2018; Jang et al., 2021). PI is a new kind of thermal insulation material, and polyimide aerogel also has the excellent thermal properties of polyimide and the characteristic of high thermal insulation of aerogel (Feng and Yu, 2021; Zhao et al., 2021; Li et al., 2022; Quan et al., 2022; Zhou et al., 2023). At the same time, PI aerogel has the two characteristics of flame retardancy and heat insulation, which can not only effectively improve the brittleness of inorganic aerogel materials and poor mechanical properties but also expand the application of organic aerogel in heat insulation and flame retardant materials (Almeida et al., 2021; Wang et al., 2022). Qian et al. (2014) used polyimide aerogels with excellent flexibility to replace traditional SiO_2 aerogels as heat insulation materials and developed polyimide aerogels with a thermal conductivity of 0.029 W/(m·k) by the supercritical CO_2 drying method. The results show that polyimide aerogel has good thermal insulation properties and flexibility, which expands the possibility of developing new polyimide aerogel insulation fabrics. Nguyen et al. (2014) used nanocellulose crystal as the strengthening material of PI aerogel, and the nanocellulose crystal filler accounted for 0–13.33% of the total solid mass fraction. Through a series of characterization tests, it was found that the enhanced material effectively improved the physical and mechanical properties of the aerogel material when the content was 560 or 920 mmol/kg.

Thermal protective clothing systems are widely used in a variety of industries, such as firefighting, automotive manufacturing, and oil rigs (Wardiningsih and Troynikov, 2021). These systems are designed to protect workers from extreme temperatures, both hot and cold. The effectiveness of thermal protective clothing is largely determined by its thermal resistance performance, flexibility, and moisture management capabilities (Li et al., 2013). Nonwoven fabrics are commonly used in such clothing systems, but they have limitations in terms of their thermal resistance and moisture management capabilities. At present, the thermal protective clothing developed and applied is relatively thick, and the heat insulation efficiency is not high, which needs to be improved (Li et al., 2021; Zhang et al., 2021). In order to make thermal protective clothing that is lightweight and has an efficient function, the development of organic aerogel/high-performance fiber wikis for composite thermal protective clothing has become the research focus (Wang, 2018). Fiber is the primary load-bearing element in the composite, and it generally remains linear elastic or perfectly plastic and becomes a stronger and stiffer material than the same when in bulk form (Mylsamy et al., 2019; Chinnasamy et al., 2020). Balu et al. prepared the fiber-reinforced composite material using natural coccidia fiber. Dynamic mechanical and thermogravimetric analyses were used to predict the effects of different fiber lengths on the dynamic mechanical properties of fiber-reinforced composites, such as loss modulus, storage modulus, and weight loss (Sethuraman et al., 2010). The combination of aerogels and high-performance fiber wikis can maximize the performance of both materials, combining the high strength of fiber wikis with the high thermal insulation and flexibility of aerogels (Li et al., 2016a; Li et al., 2016b; An et al., 2021).

In this work, we prepared a flexible PI aerogel/aramid composite material employing aramid fiber as the basis material, PI aerogel material, and a freeze-drying and softening procedure. Meanwhile, the PI aerogel/aramid composite material's thermal insulation performance was investigated, and its mechanical, flame-retardant, and thermal stability capabilities were also examined. The effects of PI aerogel containing different mass fractions on thermal insulation, flame retardancy, thermal stability, and mechanical properties of aerogel composites were studied in depth. The tensile strength and flame retardancy of neat PI aerogels are significantly enhanced by the addition of aramid fabric. The development and use of aerogel composites will benefit from the effective preparation of aramid/PI aerogel composite insulating materials.

2 Materials and methods

2.1 Materials

The aramid fiber in this study was purchased from Tianjin Glory Tang Fiber Technology Co., Ltd., China. The specifications of the purchased aramid fiber are 70 g/m^2. N, N-dimethylacetamide (DMAc), 3,3,4,4-diphenyltetracarboxylic, anhydride (BPDA), octadecylamine (ODA), triethylamine (TEA), and acetone were purchased from Sinopharm Chemical Reagent Co. Ltd., China. All the regents used in this experiment were of analytical grade purity.

2.2 Methods

2.2.1 Preparation of water-soluble PAAs

Polyamide acid (PAA), a water-soluble polymer, is used as the PI aerogel precursor material. First, a certain amount of ODA was added to a beaker and dissolved in DMAc with the mass ratio m (ODA): m (DMAc) = 1:20. Then, it was placed in an ice bath (0–4°C), and a magnetic rotor was added. The stirring speed was 500 r/min, and BPDA was added several times in a small amount. The dosage ratio of BPDA to ODA was n (BPDA) :n (ODA) = 1.1:1, and a stable yellow transparent PAA solution was obtained after reacting for 4 h. At room temperature, a certain amount of TEA was slowly dropped into the polyamide acid solution, and the dosage ratio of TEA to ODA was n (TEA) :n (ODA) = 2.5:1. After 2 h of reaction, a yellow transparent polyamide salt (PAAs) solution with a certain consistency was obtained. The prepared PAAs solution was slowly poured into a beaker containing acetone

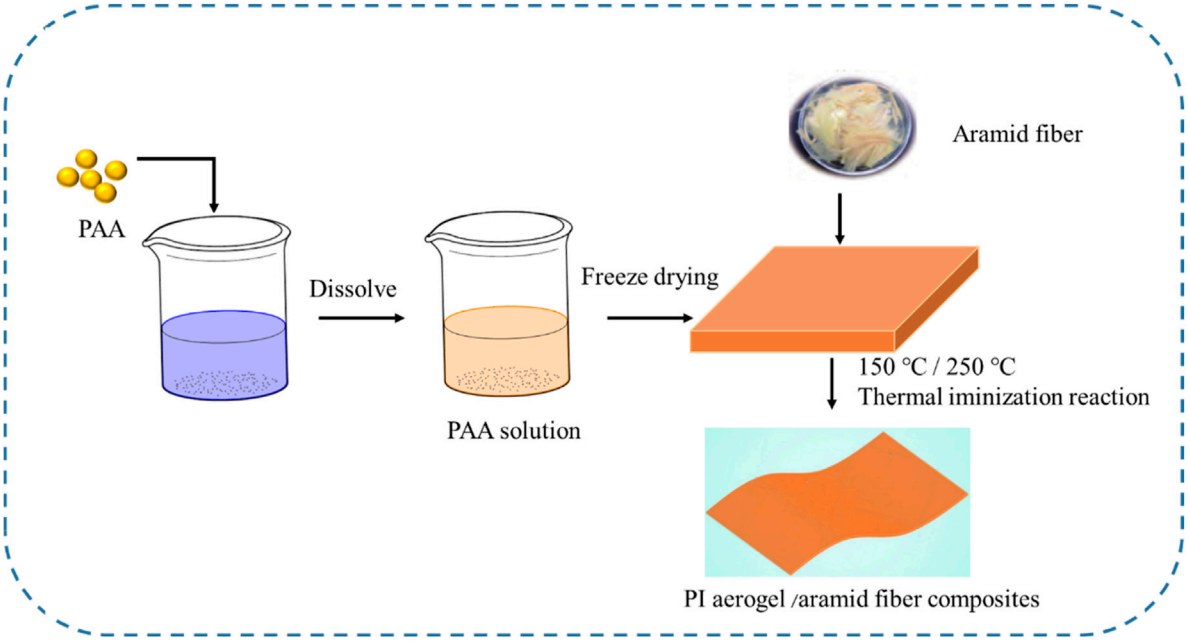

FIGURE 1
Flowchart of PI aerogel/aramid fiber composite material preparation.

and precipitated in acetone to obtain solid PAAs particles, which were fully aged in acetone and left for 3 h before being filtered out. Finally, white PAAs solid particles were obtained by drying at 45°C in an oven for 5 h to constant weight.

2.2.2 Preparation of PI aerogel/aramid fiber composites

The preparation method of PI aerogel/aramid composite is shown in Figure 1. First, the PAAs particles were added to a beaker with some deionized water and TEA, and stirred for 2 h until completely dissolved, and the PAAs aqueous solution with a solid content of 4% was obtained. It was poured into a mold with aramid non-woven fabric and frozen for 24 h. PAAs aerogel was obtained by drying under the vacuum condition of less than 3 Pa. Then, PAAs aerogel was placed into the oven for a thermal imidization reaction at 150°C for 2 h and 250°C for 1 h, and finally, PI aerogel/aramid composite was obtained. A series of PI aerogel/aramid composites were prepared by controlling the dosage of the PAAs solution. The aerogel composites with the corresponding aerogel mass fraction of 0%, 10%, and 20% were named PIA0, PIA1, and PIA2, respectively.

2.2.3 Shrinkage and porosity evaluation

The dry heat shrinkage rate refers to the percentage of length shrinkage after the PI aerogel/aramid fiber composite is treated in hot and dry air at 150 °C for 1 h. It is calculated by formula 1.

$$S = \frac{L_0 - L}{L_0} \times 100\%. \quad (1)$$

In Formula 1, S is the shrinkage rate, L_0 is the PI aerogel/aramid fiber composite length before treatment, and L is the PI aerogel/aramid fiber composite length after treatment.

The density of the PI aerogel/aramid fiber composite is calculated by calculating the diameter, length, and weight of the fiber, and the porosity is calculated by Formula 2.

$$P = \left(1 - \frac{\rho}{\rho_0}\right) \times 100\%. \quad (2)$$

In Formula 2, P is porosity, ρ is the aerogel fiber density, and ρ_0 is the composition density of the solids.

2.3 Characterizations

The microstructure of the PI aerogel/aramid composite was observed using a scanning electron microscope (SEM, SU-3500, Hitachi, Tokyo, Japan). The pore size distribution of PI aerogel/aramid fiber composites was analyzed by means of a pore size measuring instrument (CFP-1100A, American Porous Materials Corporation).

A heat conduction analyzer was used to test the thermal conductivity of PI aerogel/aramid fiber composites, and the sample size was 5 cm × 5 cm. The test temperature was 25 °C, the sampling time was 5 s, three points were collected for each sample, and the average value was taken to obtain the thermal conductivity of the samples. The thermal resistance of PI aerogel/aramid fiber composites was analyzed by dry heat, radiative heat, and contact heat resistance. The pore structure of PI aerogel/aramid fiber composites was analyzed using the Autosorb-iQ pore size distribution analyzer of Konta.

The tensile properties of PI aerogel/aramid fiber composites were tested using a universal material testing machine. The tensile strength and elongation of PI aerogel/aramid composites were characterized.

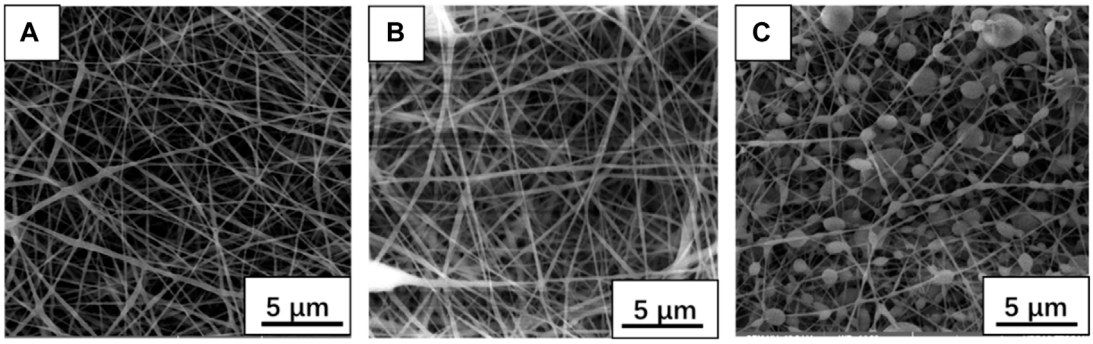

FIGURE 2
SEM image of the PI aerogel/aramid fiber composite material sample, **(A)** PIA0, **(B)** PIA1, and **(C)** PIA2.

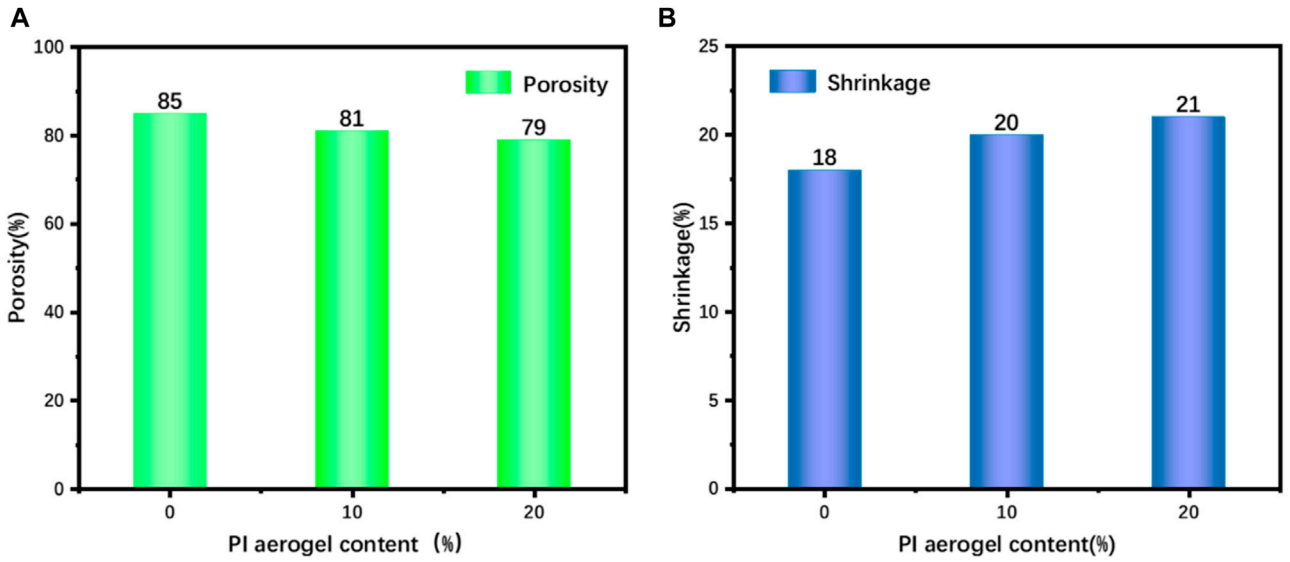

FIGURE 3
Shrinkage and porosity of the PI aerogel/aramid fiber composite material sample.

According to GB/T 24218.5-2016, the bursting strength of PI aerogel/aramid composites was tested using a microcomputer controlled electronic universal testing machine. The air permeability of the PI aerogel/aramid fiber composites samples was investigated. Air permeability was measured following the ISO 9237:1995 test method. The mean airflow was calculated from five readings for each test specimen.

3 Results and discussion

3.1 Morphology analysis of PI aerogel/aramid fiber composites

PI aerogel/aramid fiber composites were successfully prepared by the method of mold forming and freeze-drying, and the surface morphology is shown in Figure 2. The SEM images of all the samples presented a honeycomb structure and three-dimensional intersecting networks without apparent aggregation. As can be seen from Figure 2A, the thickness of the fibers is less than 1 μm. The pore size of the sample decreased slightly with the increase in the PI aerogel content, and it can be clearly seen that PI aerogel is distributed among the fibers from Figure 2C. In addition, with the increase in PI aerogel addition, the pore wall of the sample skeleton was significantly crumpled, indicating that the aramid fiber and PI aerogel in the composite aerogel formed a structure similar to "rear-concrete," and a more compact three-dimensional skeleton structure was constructed. This indicated that the improvement of the quality of PI aerogel resulted in more PI aerogel reaching the fiber skeleton structure.

Figure 3A shows the porosity of the PI aerogel/aramid fiber composite material sample. The porosity of the PI aerogel/aramid fiber composite slightly decreases from 85% to 79% with the increase in the PI aerogel content. These results indicated that the increase in the PI aerogel mass fraction significantly improved the structural integrity of the aerogel and made the PI aerogel/aramid fiber

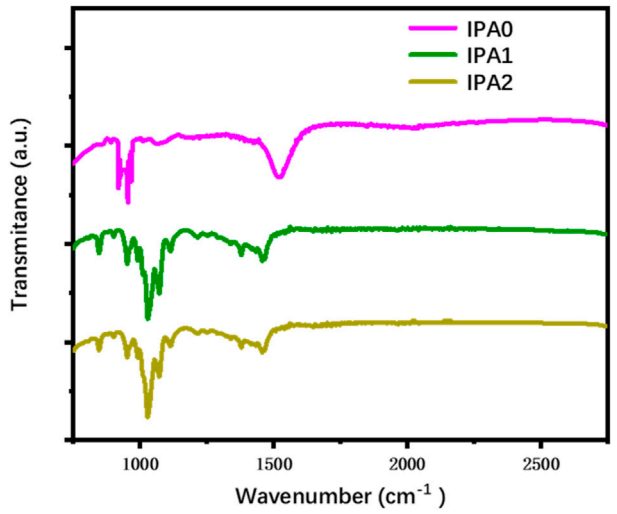

FIGURE 4
FT-IR curves of the PI aerogel/aramid fiber composite material sample.

composites have fewer pores. Figure 3B shows that the shrinkage of the PI aerogel/aramid fiber composite almost remains unchanged, and the results show that the addition of PI aerogel has little effect on the shrinkage of the PI aerogel/aramid fiber composites.

In order to explore the structure of the prepared PI aerogel/aramid fiber composite material, the infrared spectrum of the samples was tested, as shown in Figure 4. It can be observed from Figure 4 that two aramid fibers without PI aerogel were found at 1,092 and 1,613 cm^{-1}, and the characteristic peaks of PI aerogel/aramid fiber composite material supplemented with aerogel were 1,056 and 1,504 cm^{-1}, corresponding to the C=O and C-O-C stretching vibration peaks (Yang et al., 2011). In the PI aerogel/aramid fiber composite material, C=O and C-O-C stretching vibration peak to the takanami several mobile blue shift phenomenon occurred, showing that the nanometer aramid fiber surface exposed more amide groups and is conducive to the formation of hydrogen bonds between the fibers. The results show that the structural density of the aramid fiber can be improved by adding PI aerogel.

3.2 Thermal resistance of PI aerogel/aramid fiber composite

In order to test the influence of the PI aerogel mass fraction on the thermal insulation performance of composite materials, the thermal conductivity of PI aerogel/aramid fiber composite materials was tested, as shown in Figure 5A. It can be observed from Figure 5A that the PI aerogel mass fraction is positively correlated with the thermal insulation performance of the aerogel composite. The increase in the PI aerogel mass fraction will reduce the thermal conductivity of PI aerogel/aramid fiber composite and enhance the thermal insulation performance of the composite. The thermal conductivity of PIA2 is as low as 0.031 W/(m·k), compared with 0.047 W/(m·k) of aramid fiber PIA0. This is because the microporous structure of aerogel limits the flow of air and extends the heat conduction path, thus limiting the role of heat convection and heat conduction in the process of heat transfer.

To further determine the thermal insulation properties of the PI aerogel/aramid composite, the thermal radiation resistance was measured. The PI aerogel/aramid composites were tested by exposing them to a 250°C heat source at a distance of 20 cm, and the increase in the PI aerogel/aramid composite temperature with time was recorded.

The curve of PI aerogel/aramid composites temperature change over time is shown in Figure 5B.

It has been found that IPA2 has the maximum resistance to radiant heat of the PI aerogel/aramid composite, and it warms up the slowest over time. When the temperature of the PI aerogel/aramid composite rises to 45°C, the individual wearing it will feel pain, and when the temperature rises to 55°C, it will cause burns to the human body (Shaid et al., 2021). The time to reach the temperature that would cause pain and burn for IPA2 is recorded as 587 s and 960 s, while the time to reach the temperature that would cause pain and burn for IPA0 is recorded as 358 s and 591 s. The results showed that the PI aerogel/aramid composites containing more PI aerogel mass fraction showed better thermal insulation performance.

3.3 PI aerogel/aramid composite physical properties

The tensile property is essential for the application of PI aerogel/aramid fiber composite (Zhuo et al., 2020), so the PI aerogel/aramid composite tensile test was carried out, and the stress–strain curve is shown in Figure 5A. As can be seen from Figure 6A, the tensile strength of PI aerogel/aramid fiber composites increases with the increase in the PI aerogel mass fraction. In addition, due to the crosslinking effect of aerogel, the elongation at the break of PI aerogel/aramid composite was significantly higher than that of the aramid fiber, indicating that the addition of IP aerogel was helpful in improving the flexibility of the aramid fiber. This is because the synergistic action of aerogel reduces the sliding friction between the fibers inside the PI aerogel/aramid fiber composite material, which makes it easier to deform after receiving the force and improves the softness of the material. Figure 6B shows the bursting strength of the PI aerogel/aramid fiber composite; IPA0 showed the minimum strength of 736 kPa, and IPA2 demonstrated a maximum strength of 798 kPa. The strength of the PI aerogel/aramid fiber composite was gradually improved with the increment of the PI aerogel content. The flexibility of PI aerogels/aramid composites was characterized by the crease recovery angle test. The smaller the crease recovery angle, the better the flexibility of the materials. As can be seen from Figure 6C, with the increase in the PI aerogel content, the crease recovery angle of PI aerogel/aramid composite decreases significantly from 145° of PIA0 to 124° of PIA2. The reason is that after the aerogel material is subjected to external force, the relative movement between the fibers causes the stress to be released and changes to a stable state. After the external force is removed, the recovery force decreases, so the crease recovery angle becomes smaller.

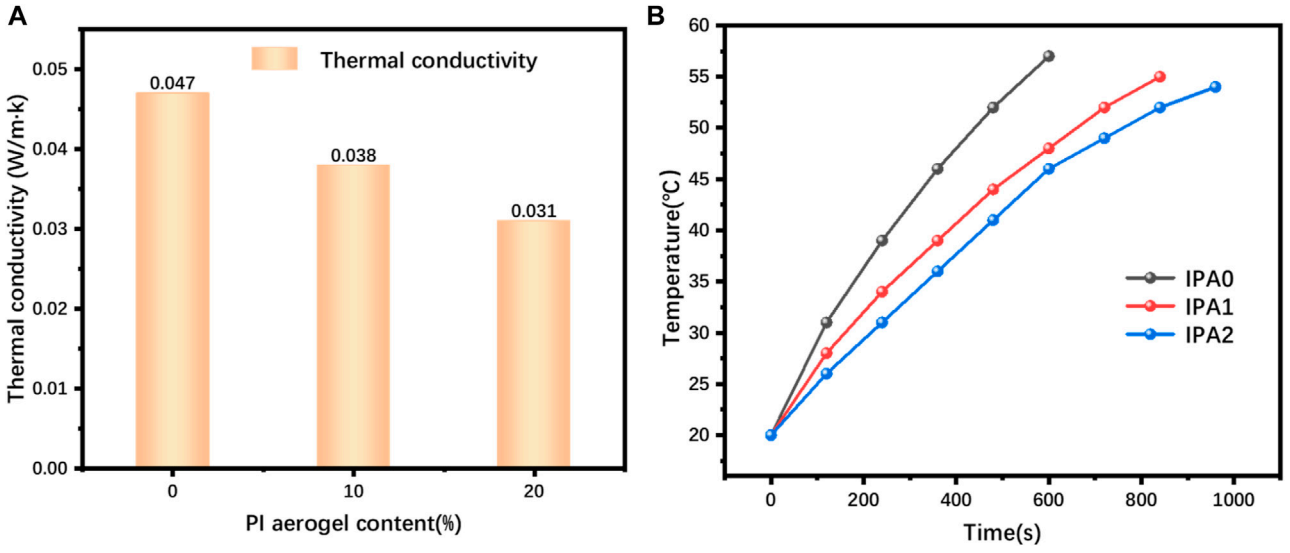

FIGURE 5
(A) PI aerogel/aramid fiber composite's thermal conductivity and **(B)** resistance of the PI aerogel/aramid composite against radiant heat exposure.

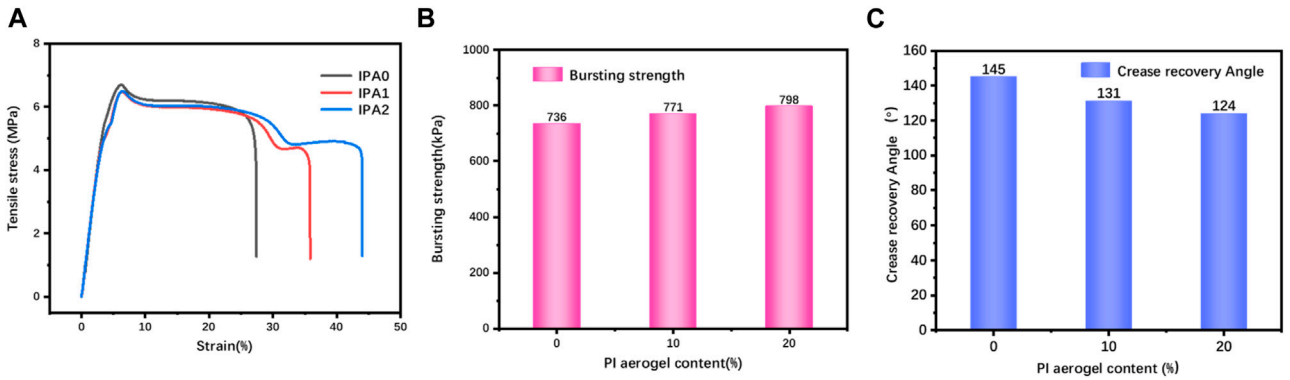

FIGURE 6
(A) Stress–strain curves of PI aerogel/aramid fiber composite, **(B)** bursting strength of PI aerogel/aramid fiber composite, and **(C)** crease recovery angle of PI aerogel/aramid fiber composite.

3.4 PI aerogel/aramid fiber composite clothing thermal comfort

Because the PI aerogel/aramid fiber composite is used in protective clothing fabrics, wearing comfort is also particularly important. The thermal comfort of clothing material is directly related to its air permeability, moisture permeability, and heat preservation. The air permeability of clothing materials is particularly important, which directly affects the evaporation of human sweat and skin respiration (Awais et al., 2021). We tested the air permeability of the PI aerogel/aramid fiber composite, and the test results are shown in Figure 7A. We can observe that the permeability of the control fabric without IP aerogel is significantly higher than that of IPA1 and IPA2. For IPA0, the maximum permeability to air is 35.1 mL cm^{-2} s^{-1} at 100 Pa, and for IPA2 with 20% aerogel content, the minimum air permeability is 24.8 mL cm^{-2} s^{-1} at 100 Pa. The air permeability of textile materials is directly related to its porosity. The results showed that the presence of IP aerogel particles blocked the free flow of air and blocked the pores between the aramid fibers, therefore decreasing the permeability of the PI aerogel/aramid fiber composite. Considering the air permeability and moisture permeability required by the aramid fabric, the low resistance to moisture vapor transmission with high air permeability is foreseeable. So, PI aerogel/aramid fiber composite will certainly be able to provide better thermal comfort than the aramid fiber.

In addition, for PI aerogel/aramid fiber composite materials used in clothing fabrics, the moisture permeability index (i_{mt}) for assessing clothing thermal comfort is also significant. The i_{mt} value is based on the measurement method of the heat insulation value of clothing. It is used to measure the i_{mt} value of clothing when the human skin is completely wet. The PI aerogel/aramid fiber composite of the moisture

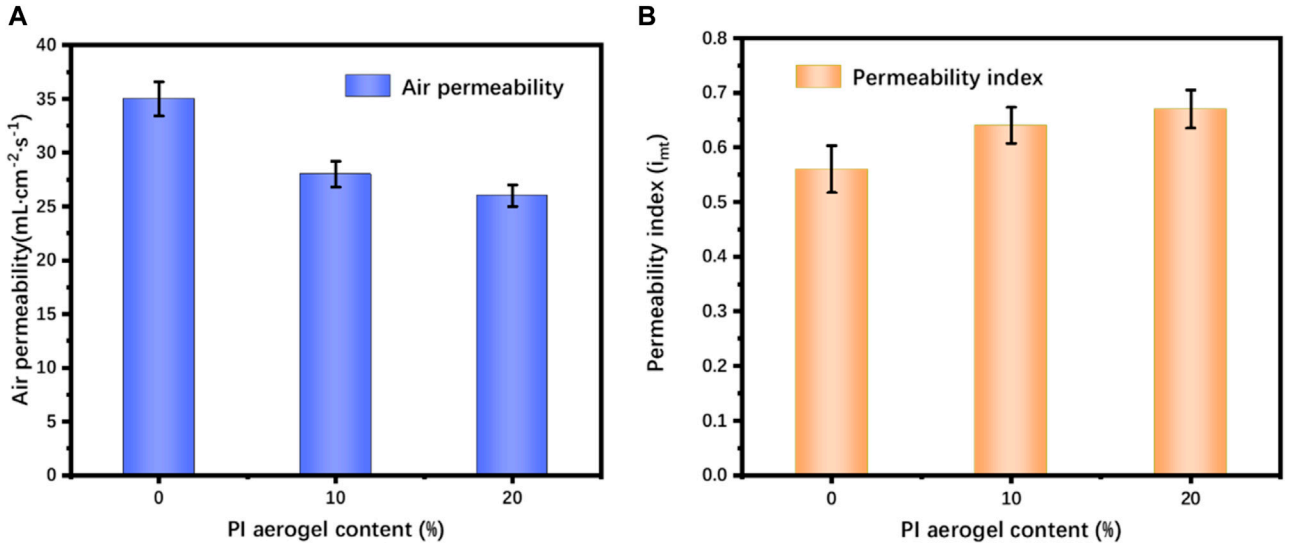

FIGURE 7
(A) Air permeability and **(B)** moisture permeability index of PI aerogel/aramid fiber composite.

permeability index value is shown in Figure 7B. From Figure 6B, it can be observed that the lowest i_{mt} value of IPA0 without IP aerogel is 0.558, and the highest value of i_{mt} is 0.679. In general, the i_{mt} value of the clothing material will increase with the increase in ambient temperature and humidity to maintain the heat balance. Therefore, the larger the i_{mt} value of clothing material, the easier it is to maintain the thermal balance of human body in a high temperature and humidity environment. This high-permeability PI aerogel/aramid fiber composite will provide better thermal comfort for the wearer in a high temperature and humidity environment.

4 Conclusion

In summary, microporous PI aerogel/aramid composites with robust mechanical properties and highly efficient heat insulation performance were prepared by molding and freeze-drying. With the increase in the PI aerogel mass fraction, PI aerogel/aramid fiber composite material shows better thermal insulation performance. PIA2 has the best thermal insulation, with a thermal conductivity as low as 0.031 W/(m·k) at room temperature. In addition, the thermal insulation properties of the PI aerogel/aramid fiber composites were also significantly improved with the increase in the PI aerogel mass fraction. The thermal conductivity of the composites was significantly reduced due to the high porosity and low thermal conductivity of PI aerogel. Furthermore, the PI aerogel/aramid fiber composite with 20% PI aerogel mass fraction has the best deformation performance while maintaining high tensile strength. In addition, for the PI aerogel/aramid fiber composite with 20% PI aerogel mass fraction, the air permeability is 24.8 mL cm^{-2} s^{-1} at 100 Pa and the permeability index value is 0.679. The results indicate that the use of aerogel nonwoven fabric in thermal protective clothing systems is a viable alternative to commercial nonwoven fabrics. Its superior thermal resistance performance, flexibility, and moisture management capabilities make it a potentially ideal material for such systems. Further research is needed to explore the use of the fabric in different work environments to determine its effectiveness and potential limitations. It can provide the material basis for the development of fire protection clothing, petrochemical fire protection clothing, and heat protection clothing with lightweight and efficient heat insulation function.

Data availability statement

The original contributions presented in the study are included in the article/supplementary material; further inquiries can be directed to the corresponding author.

Author contributions

YL: conceptualization, methodology, investigation, formal analysis, and writing—original draft; DW: data curation and writing—original draft; JL: resources, supervision, and writing—review and editing.

Funding

Theoretical and Experimental Study on Heat and Mass Transfer of Physalis pubescens Modified Atmosphere Preservation (Fund Projects Number: LH2023E027).

Conflict of interest

The authors declare that the research was conducted in the absence of any commercial or financial relationships that could be construed as a potential conflict of interest.

Publisher's note

References

Adhikary, S. K., Ashish, D. K., and Rudžionis, Ž. Y. (2021). Aerogel based thermal insulating cementitious composites: A review. *ENERGY Build.* 245, 111058. doi:10.1016/j.enbuild.2021.111058

Ageev, B. G., and Ponomarev, Y. N. (2018). Estimate of methane-capacity of aerogel samples of different compositions. *24TH Int. SYMPOSIUM Atmos. OCEAN Opt. Atmos. Phys.* 15, doi:10.1117/12.2503956

Almeida, C. M. R., Ghica, M. E., Ramalho, A. L., and Durães, L. (2021). Silica-based aerogel composites reinforced with different aramid fibres for thermal insulation in Space environments. *J. Mater. Sci.* 56 (24), 13604–13619. doi:10.1007/s10853-021-06142-3

An, L., Liang, B., Guo, Z., Wang, J., Huang, Y., et al. (2021). Wearable aramid-ceramic aerogel composite for harsh environment. *Adv. Eng. Mater.* 23 (3). doi:10.1002/adem.202001169

Awais, M., Krzywinski, S., and Wendt, E. (2021). A novel modeling and simulation approach for the prediction of human thermophysiological comfort. *Text. Res. J.* 91 (5-6), 691–705. doi:10.1177/0040517520955227

Cao, C., and Yuan, B. (2021). Thermally induced fire early warning aerogel with efficient thermal isolation and flame-retardant properties. *Polym. Adv. Technol.* 32 (5), 2159–2168. doi:10.1002/pat.5246

Chinnasamy, V., Pavayee Subramani, S., Palaniappan, S. K., Mylsamy, B., and Aruchamy, K. (2020). Characterization on thermal properties of glass fiber and kevlar fiber with modified epoxy hybrid composites. *J. Mater. Res. Technol.* 9 (3), 3158–3167. doi:10.1016/j.jmrt.2020.01.061

Dai, J. P., Li, D., Du, S., Cao, Z. W., and Xu, X. L. (2021). STUDY ON THE THERMAL INSULATION PROPERTY OF SiO2 AEROGEL INFLUENCED BY THE PHENOLIC RESIN PYROLYSIS GAS PERMEATION. *HEAT Transf. Res.* 52 (13), 55–72. doi:10.1615/heattransres.2021038627

Du, Y., and Kim, H.-E. (2019). A market research on the development trends of aerogel daily clothing. *Fash. Text. Res. J.* 21 (1), 96–103. doi:10.5805/sfti.2019.21.1.96

Du, Y., and Kim, H. E. (2022). Research trends of the application of aerogel materials in clothing. *Fash. Text.* 9 (1), 23. doi:10.1186/s40691-022-00298-5

Fan, W., Zuo, L., Zhang, Y., Chen, Y., and Liu, T. (2018). Mechanically strong polyimide/carbon nanotube composite aerogels with controllable porous structure. *Compos. Sci. Technol.* 156, 186–191. doi:10.1016/j.compscitech.2017.12.034

Feng, C., and Yu, S.-S. (2021). 3D printing of thermal insulating polyimide/cellulose nanocrystal composite aerogels with low dimensional shrinkage. *POLYMERS* 13 (21), 3614. doi:10.3390/polym13213614

Ivanov, N. N., and Ivanov, A. N. (2014). A sensor for the spatial registration and measurement of particles parameters in near and deep space-Experimental investigation of SiO2-aerogel characteristics. *Sol. Syst. Res.* 48 (7), 549–554. doi:10.1134/s0038094614070090

Jang, D., Yoon, H. N., Seo, J., Lee, H., and Kim, G. (2021). Effects of silica aerogel inclusion on the stability of heat generation and heat-dependent electrical characteristics of cementitious composites with CNT. *Cem. Concr. Compos.* 115, 103861. doi:10.1016/j.cemconcomp.2020.103861

Laskowski, J., Milow, B., and Ratke, L. (2015). The effect of embedding highly insulating granular aerogel in cellulosic aerogel. *J. Supercrit. FLUIDS* 106, 93–99. doi:10.1016/j.supflu.2015.05.011

Lee, K.-Y., Nah, H.-Y., Choi, H., Parale, V. G., and Park, H. H. (2018). Methyltrimethoxysilane silica aerogel composite with carboxyl-functionalised multi-wall carbon nanotubes. *Int. J. Nanotechnol.* 15 (6-7), 587–597. doi:10.1504/ijnt.2018.096349

Lee, Y. J., Jung, J. C., Park, S., Seo, J. G., Baeck, S. H., Yoon, J. R., et al. (2011). Effect of preparation method on electrochemical property of Mn-doped carbon aerogel for supercapacitor. *Curr. Appl. Phys.* 11 (1), 1–5. doi:10.1016/j.cap.2010.06.001

Lei, F., Chao, C., Chen-dong, W., Mo, Z., Jing, W., Wei, Q., et al. (2006). Experiment study on the moisture absorption and desorption characteristic of SiO2-aerogel. *J. Build. Mater.* 9 (5), 517–520.

Lei, Y., Wang, M., Chen, X., Hu, Z., and Song, H. (2018). Polyimide/silica aerogel flexible composite film with high thermal insulation and good mechanical strength. *RARE METAL Mater. Eng.* 47, 242–245.

Li, J., Zhang, L., Pang, Y., Wang, X., Bai, B., Zhang, W., et al. (2022). Polyimide composite aerogels towards highly efficient microwave absorption and thermal insulation. *Compos. PART A-APPLIED Sci. Manuf.* 161, 107112. doi:10.1016/j.compositesa.2022.107112

Li, X., Dong, G., Liu, Z., and Zhang, X. (2021). Polyimide aerogel fibers with superior flame resistance, strength, hydrophobicity, and flexibility made via a universal sol-gel confined transition strategy. *ACS NANO* 15 (3), 4759–4768. doi:10.1021/acsnano.0c09391

Li, X.-X., Sun, Y.-C., Xu, J.-Y., and Chen, R. X. (2013). Thermal requirement analysis of phase change protective clothing in low temperature environment. *SILK, Prot. Cloth. ECO-TEXTILES* 796, 649–652. doi:10.4028/www.scientific.net/AMR.796.649

Li, Z., Cheng, X., He, S., Shi, X., Gong, L., and Zhang, H. (2016a). Aramid fibers reinforced silica aerogel composites with low thermal conductivity and improved mechanical performance. *Compos. PART A-APPLIED Sci. Manuf.* 84, 316–325. doi:10.1016/j.compositesa.2016.02.014

Li, Z., Gong, L., Li, C., Pan, Y., Huang, Y., and Cheng, X. (2016b). Silica aerogel/aramid pulp composites with improved mechanical and thermal properties. *J. NON-CRYSTALLINE SOLIDS* 454, 1–7. doi:10.1016/j.jnoncrysol.2016.10.015

Liu, F., Wang, X., Li, Y., Ren, M., He, P., Wang, L., et al. (2022). Dendrimer-modified gelatin methacrylate hydrogels carrying adipose-derived stromal/stem cells promote cartilage regeneration. *Aerosp. Mater. Technol.* 52 (2), 26–47. doi:10.1186/s13287-022-02705-6

Mylsamy, B., Palaniappan, S. K., Pavayee Subramani, S., Pal, S. K., and Aruchamy, K. (2019). Impact of nanoclay on mechanical and structural properties of treated Coccinia indica fibre reinforced epoxy composites. *J. Mater. Res. Technol.* 8 (6), 6021–6028. doi:10.1016/j.jmrt.2019.09.076

Nguyen, B. N., Cudjoe, E., Douglas, A., Scheiman, D., McCorkle, L., Meador, M. A. B., et al. (2014). Polyimide cellulose nanocrystal composite aerogels. *Abstr. Pap. Am. Chem. Soc.* 248. doi:10.1021/acs.macromol.5b01573

Qian, J., Chen, Y., Feng, J., et al. (2014). Synthesis and properties of polyimide aerogels. *J. Funct. Mater.* 45 (20), 20122–20126.

Quan, Z., Wang, Q., Piao, C., Tang, Y., Chen, Y., and Zhao, N. (2022). Preparation and mechanism of SiO2 aerogel gypsum based materials. *Integr. Ferroelectr.* 228 (1), 67–78. doi:10.1080/10584587.2022.2072123

Sethuraman, B., Subramani, S. P., Palaniappan, S. K., Mylsamy, B., and Aruchamy, K. (2010). Quotation3.pdf. https://zh.wikihow.com/.

Shaid, A., Bhuiyan, M. A. R., and Wang, L. (2021). Aerogel incorporated flexible nonwoven fabric for thermal protective clothing. *Fire Saf. J.* 125, 103444. doi:10.1016/j.firesaf.2021.103444

Stan, L., Malutan, T., Volf, I., Popa, M., Tincu, C. E., and Stan, C. S. (2022). Photoluminescent polymer aerogels with R, G and B emission. *[J/OL]* 23 (24), 16004. doi:10.3390/ijms232416004

Wang, J.-M. (2018). Preparation and properties of SiO2 aerogel and fabric composite based on polyurethane. *Integr. Ferroelectr.* 189 (1), 36–43. doi:10.1080/10584587.2018.1454801

Wang, Z., Liu, X., Tai, J., and Tang, W. (2022). Application of weighted gene co-expression network analysis to identify novel key genes in diabetic nephropathy. *Mod. Chem. Ind.* 42 (2), 112–124. doi:10.1111/jdi.13628

Wardiningsih, W., and Troynikov, O. (2021). Effects of hip protective clothing on thermal wear comfort of clothing ensembles. *Res. J. Text. Appar.* 25 (3), 226–239. doi:10.1108/rjta-11-2020-0124

Yang, M., Cao, K., Sui, L., Qi, Y., Zhu, J., Waas, A., et al. (2011). Dispersions of aramid nanofibers: A new nanoscale building block. *ACS NANO* 5 (9), 6945–6954. doi:10.1021/nn2014003

Zhang, B., Wu, P., Zou, H., and Liu, P. (2018b). Morphology and properties of polyimide/multi-walled carbon nanotubes composite aerogels. *High. Perform. Polym.* 30 (3), 292–302. doi:10.1177/0954008317693072

Zhang, D., Lin, Y., Wang, W., Li, Y., and Wu, G. (2021). Mechanically strong polyimide aerogels cross-linked with dopamine-functionalized carbon nanotubes for oil absorption. *Appl. Surf. Sci.* 543, 148833. doi:10.1016/j.apsusc.2020.148833

Zhang, R., An, Z., Zhao, Y., Zhang, L., and Zhou, P. (2020). Nanofibers reinforced silica aerogel composites having flexibility and ultra-low thermal conductivity. *Int. J. Appl. Ceram. Technol.* 17 (3), 1531–1539. doi:10.1111/ijac.13457

Zhao, F., Zhu, J., Peng, T., Liu, H., Ge, S., Xie, H., et al. (2021). Preparation of functionalized halloysite reinforced polyimide composite aerogels with excellent thermal insulation properties. *Appl. CLAY Sci.* 211, 106200. doi:10.1016/j.clay.2021.106200

Zhou, J., Liu, X., He, X., Wang, H., Ma, D., and Lu, X. (2023). Bio-inspired aramid Fibers@silica binary synergistic aerogels with high thermal insulation and fire-retardant performance. *J/OL]* 15 (1), 141. doi:10.3390/polym15010141

Zhuo, L., Ma, C., Xie, F., Chen, S., and Lu, Z. (2020). Methylcellulose strengthened polyimide aerogels with excellent oil/water separation performance. *CELLULOSE* 27 (13), 7677–7689. doi:10.1007/s10570-020-03311-6

Ze, Z., Xiaodong, W., Yu, W., Wenbing, Z., Xueling, W., Jun, S., et al. (2018a). Aerogels and their applications - a short review. *J. Chin. Ceram. Soc.* 46 (10), 1426–1446.